Desalination and Water Treatment
www.deswater.com

doi: 10.5004/dwt.2019.23821

151 (2019) 34–46
May

Energy management of nuclear desalination plant by efficient coupling a pressurized water reactor and a multi-effect distillation system – thermodynamic evaluation

A. Naserbegi, A. Rezaei, Gh. Alahyarizadeh*, M. Aghaie

Engineering Department, Shahid Beheshti University, G.C., P.O. Box 1983969411, Tehran, Iran, Tel. +98 21 29904226; email: g_alahyarizadeh@yahoo.com (Gh. Alahyarizadeh), naserbeigi90@yahoo.com (A. Naserbegi), arezaey90@gmail.com (A. Rezaei), mahdi.aghaie2003@gmail.com (M. Aghaie)

Received 30 June 2018; Accepted 21 January 2019

ABSTRACT

Thermodynamic evaluation of a nuclear desalination plant by coupling a pressurized water reactor and a multi-effect distillation system was performed by using a new version of the Desalination Thermodynamic Optimization Program. For energy management of a nuclear desalination plant, all possible coupling configurations between the nuclear power plant and the desalination process were investigated. The software was upgraded to study exergy analysis by adding related exergy equations. Several important output parameters, such as power loss ratio, net efficiency, thermal utilization, and total power requirement, were compared; these parameters varied from 8.7% to 28.5%, 32.6% to 33.3%, 36.1% to 36.9% and 14.7 to 35.3 MWe, respectively. The minimum power loss ratio and the maximum net efficiency and thermal utilization were obtained from multi-extraction points, which included the heat rejected by the condenser. Exergy analysis showed that the maximum exergy destructions (1,292.9 MWth) were related to the reactor core, which is considered the main irreversible component. The results demonstrated good agreement with previous theoretical and experimental studies.

Keywords: Nuclear desalination plant; Pressurized water reactor; Multi-effect distillation; Thermodynamic evaluation; Exergy analysis; DE-TOP

1. Introduction

Humanity and the environment are facing the crucial problem of freshwater scarcity [1,2]. Freshwater constitutes only 2.5% of the 70% of the water that covers the earth. Nearly less than 0.008% of the estimated freshwater or approximately 70,000 km^3 is readily accessible for human use [3–6]. Seawater desalination is an important method that can be applied to overcome the water crisis and the freshwater shortage. Seawater desalination technology has been established since the middle of the twentieth century and is widely developed in many countries, specifically in the Middle East and South Africa [6–10]. Commercial and industrial desalination processes are mainly categorized into (a) thermal methods, which use heat energy, and (b) membrane processes, which employ electrical or mechanical power for distillation. Thermal processes are mostly based on multi-stage flash (MSF) and multi-effect distillation (MED), and membrane processes are based on reverse osmosis (RO) and electrodialysis [11–13]. Similar to other industrial technologies, desalination technology requires energy inputs. Input energies based on fossil energy resources affect the environment through CO_2 emissions. Furthermore, providing energy based on fossil resources entails additional costs related to transportation and other activities [11]. In addition to fossil fuels, renewable energy sources such as solar energy are used as energy sources for the desalination process. Solar energy has several advantages, including being a form

* Corresponding author.

of free energy and requiring relatively low operating costs, simple assembly and operation, and moderately low overhaul and maintenance costs. However, solar energy-based desalination plants have some disadvantages. The availability of solar radiation is a vital issue related to the use of solar energy for desalination plants. Solar desalination plants are suitable for geographical places with considerable solar radiation. Geographical and weather conditions play substantial roles in the solar plant operation. Moreover, due to low efficiency, solar energy plants have to couple with much smaller-capacity desalination plants [14,15].

Nuclear energy is one energy source that is currently playing a major role in electrical and thermal energy generation. Nearly 17% of the world's electricity is produced through nuclear energy. Nuclear energy is safe, economical, and reliable, and it has minimum effects on the environment [16]. The combined heat and power mode operation of nuclear power plants (NPPs) raises energy conversion efficiencies considerably [17]. Although, NPPs are primarily used for electricity generation, some of the first nuclear reactors were established for heat supply. More than 60 nuclear reactors currently operate as heat supply for industrial processes, including seawater desalination technologies [16]. The International Atomic Energy Agency (IAEA) defines the use of electrical and/or thermal nuclear energy in the desalination process or nuclear desalination as "the production of potable water from seawater in a facility in which a nuclear reactor is used as the source of energy for the desalination process" [9]. Therefore, three technologies constitute nuclear desalination, namely, nuclear technology, desalination technology, and a system for coupling these technologies [18]. IAEA has continuously supported and addressed the main considerations concerning any activities in the field of nuclear desalination over the last three decades. In this regard, several studies have been published by IAEA on different related areas, including economic evaluation [6,19,20], safety consideration [21], and technical aspects [22–25] of nuclear desalination. The Desalination Economic Evaluation Program (DEEP) was a key outcome of the economic evaluation process and was developed to estimate the installation and operation costs of nuclear desalination plants constructed by various desalination systems and diverse energy sources, including fossil and nuclear energy. DEEP is software that is continuously under development and verification, and it can calculate water and power costs by solving a detailed economic model [15,20].

A new thermodynamic model called Desalination Thermodynamic Optimization Program (DE-TOP) was recently released by IAEA to address this issue. DE-TOP is a powerful Excel-based tool for simulating and analyzing the different conditions of coupling between the water/steam cycle of nuclear power reactors and seawater desalination plants. DE-TOP analyzes and compares the performance of various coupling options of nuclear power reactors and desalination plants from a thermodynamic perspective. A wide overview of both thermodynamic and economic aspects of nuclear power desalination is provided by DE-TOP along with DEEP [26].

Hafdhi et al. [27] exergo-economically optimized a double-effect thermal desalination plant to be used in an industrial steam power plant. The desalination plant was coupled with the thermal power unit of a phosphoric acid factory to produce about 528 m^3 of fresh water. The foremost object of this research is to express the optimum operating conditions required to reach the maximum exergy efficiency with minimum production cost. The maximum exergy efficiency obtained for the evaporator (82%) and the condenser presented the lowest exergy efficiency (31.66%). Ali Hosseini et al. [28] illustrated an operational example of using solar energy for desalination by coupling an active solar distillation system with a vacuum-type heat exchanger. The system was developed by using a solar parabolic concentrator and a linear solar absorber. They experimentally evaluated the system from 10 am to 2:30 pm on five sunny days in October 2015. They reported a maximum distilled water of 1.5 $kg/m^2/d$ by considering 1,227.68 W/m^2 of average solar radiation and a heat exchanger vacuum pressure of 0.5 bar. They also achieved maximum energy and exergy efficiencies of 60.98% and 56.80% for the heat exchanger on the second day. Their results indicate that total solar radiation was the most significant parameter that influenced the temperature of oil entering the heat exchanger. Ming et al. [29] provided a numerical analysis of seawater desalination based on the use of a solar chimney power plant. They numerically investigated the performance of a desalination plant by considering a plant variant with the same size as the Manzanares pilot model. Their results indicated that the fresh water output increases by increasing the amount of water sprayed, which is the principal parameter in improving the desalination efficiency of the plant. An economical comparative study of nuclear power desalination using two different pressurized water reactors (PWR) was performed by Alonso et al. [30] they investigated the cogeneration of potable water and electricity from desalination plants based on different nuclear reactors, that is, big and small/medium reactors. They further studied alternatives based on the use of three different desalination processes, namely, MED, MSF, and RO, including the two other hybrid methods. Dincer and Dincer et al. [31] performed a comparative evaluation study on possible desalination options coupled with various NPPs. Their evaluation was conducted for different types of desalination methods such as MED, MSF, RO and hybrid with steam cycle-, gas cycle-, and combined cycle-based NPPs. They employed DEEP to assess the costs of water production for each scenario. Their results indicated that MED with a gas turbine-based NPP presents the lowest fresh water cost of $\$0.71/m^3$. Mansouri and Ghoniem [32] compared nine different scenarios of the establishment of a desalination plant in Saudi Arabia by using the DEEP modeling tool. They focused on economic evaluation of fossil fuel- and nuclear-based desalination plants. The case study was conducted on the Al Khobar plant, which is owned by SWCC of Saudi Arabia. This plant is located on the east coast of Saudi Arabia and produces 2,80,000 m^3/d of water. They showed that the nuclear options provided by DEEP are much more cost-effective than the fossil fuel option and therefore makes economic sense for Saudi Arabia.

Li et al. [33] also investigated and compared the coupling of a 200 MW integrated nuclear heating reactor with the following three desalination processes: (i) low-temperature horizontal tube evaporator MED (TVC-MED), (ii) high-temperature vertical tube evaporator (VTE-MED), and (iii) a hybrid of RO and MED. Their economic analysis results showed that the hybrid of RO and MED has the best economic

competitiveness. Abdoelatef et al. [9] thermodynamically evaluated the coupling of an advanced pressurized reactor with a thermal desalination plant via DE-TOP. They employed a range of thermal desalination technologies, including (i) MSF, (ii) MED, and (iii) hybrid MED and thermal vapor compression (MED-TVC). Their results showed that the net efficiency is strongly dependent on the extraction positions. Sanchez-Cervera et al. also [26] used DE-TOP to analyze various coupling configurations between an NPP and a desalination plant, including various alternatives of steam extractions. Their study shows the advantages and disadvantages of each coupling option. Elaskary estimated power and water costs for several coupled nuclear reactors (PWR, PHWR, and BWR) with three main desalination processes (MED, MSF, and RO) and two hybrid plants (MED+RO and MSF+RO) by using DEEP. His thermodynamic analysis for various coupled plants was performed by using DE-TOP.

Although, the above studies show the various alternatives of coupling between NPPs and desalination processes, a new optimized and efficient design that couples steam extractions and the desalination plant has yet to be proposed. This paper describes the structure and outstanding features of DE-TOP and presents a thermodynamic comparison of different coupling options, including various alternatives for steam extractions and multiple-steam extraction and desalination processes. The freely distributed DE-TOP V2 beta used in this study is under a license agreement (http://www.iaea.org/NuclearPower/Desalination/).

1.1. DE-TOP models and simulation parameters

DE-TOP is a user-friendly Microsoft Excel-based program written in Visual Basic and is used as a tool for thermodynamic evaluation and optimization of desalination plants, such as nuclear desalination plants. The water steam cycle of various water-cooled plants, including nuclear and fossil fuel-based plants, and coupling configurations between any non-electrical applications are modeled by using DE-TOP. Energy flows and energy of the different parts of the cogeneration system are calculated by using DE-TOP [26,34,35]. The DE-TOP structure comprises three main modules, namely, the graphical user interface (GUI) by which a user can load input data and observe outputs, the processing modules in which all calculations related to the power plant and the cogeneration system are performed, and the data module that handles the proceeding module by using its library. From another perspective, the DE-TOP operation consists of four main steps, which are shown in Fig. 1. Through interactive controls, a user can input data and describe the case of the study [34].

The power plant is defined in the first step and simulated as a single-purpose plant, such as for electricity production only. Then, this power plant is modified to analyze its performance when it is used as a cogeneration plant. A non-electrical application, such as thermal desalination or heating circuit, is defined to couple with the power plant in the second step. Afterwards, the coupling configuration between the power plant and the non-electrical application is selected. Finally, the simulation is run, and output data are collected in a detailed report as the calculation results [34,36].

The energy and exergy flows of the cogeneration system were calculated by DE-TOP. However, the possibility of calculating the exergy parameters for each component of the power plant does not exist. Energy analysis does not give any information about the system's internal losses; thus, it cannot interpret thermodynamic evaluations of the systems and processes. Therefore, to calculate the exergy efficiency and exergy destruction for components of the system, exergy equations should be added to the software. The energy balance equation (first law of thermodynamics) for each component of the power plant is

$$\dot{Q}-\dot{W}=\sum_{e}\dot{m}_{e}\left(h_{e}+\frac{V_{e}^{2}}{2}+gz_{e}\right)-\sum_{i}\dot{m}_{i}\left(h_{i}+\frac{V_{i}^{2}}{2}+gz_{i}\right) \tag{1}$$

Physical exergy for each flow is obtained from Eq. (2).

$$E=\left(H-H_{0}\right)-T_{0}\left(S-S_{0}\right) \tag{2}$$

The reference state is chosen as the subcooled liquid at a temperature of 24°C and a pressure of 1 bar for streams. The exergy balance equation (second law of thermodynamics) for each part of the power plant is expressed as [37–39]

$$\dot{E}_{Q}-\dot{W}+\sum_{\text{in}}\dot{m}_{\text{in}}e_{\text{in}}-\sum_{\text{out}}\dot{m}_{\text{out}}e_{\text{out}}=\dot{E}_{D} \tag{3}$$

The list of added equations to DE-TOP is given in Table 1.

Fig. 2 shows the GUI of the power plant model definition with a new version of DE-TOP V2 called DE-TOPb. The power plant is chosen as an alternative from the predefined cases. Several input parameters are required to define the NPP, such as steam generator parameters, reheat, feed water line, and cooling system parameters, component efficiencies, and feed water preheating line (pressure of steam extraction to preheaters). The NPP parameters used in this simulation were obtained from reference [26] and summarized in Table 2.

The type of desalination technology, the desalination plant capacity, the total dissolved solids (TDS) in seawater or seawater TDS, and the maximum brine temperature are the essential parameters of the desalination plant required to simulate the desalination system. The desalination plant parameters used in this simulation are listed in Table 3.

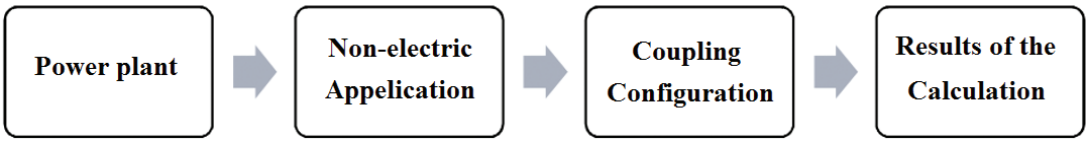

Fig. 1. General DE-TOP program layout.

Table 1
Main equations for energy and exergy analyzes for the power plant [37]

Components	Equations	
Turbines		
Energy balance	$\dot{W}_t = \left(\dot{W}_u\right)_t = \sum_i \dot{m}_i h_i - \sum_e \dot{m}_e h_e$	(4)
Exergy destruction	$\sum \dot{E}_{\text{in}} - \sum \dot{E}_{\text{out}} = \dot{W}_T + \dot{E}_D$	(5)
Exergy efficiency	$\varepsilon_t = \frac{\dot{W}_t}{\sum_i \dot{E}_i - \sum_e \dot{E}_e}$	(6)
Pumps		
Energy balance	$\dot{W}_p = \dot{m}_i h_i - \dot{m}_e h_e$	(7)
Exergy destruction	$\sum \dot{E}_{\text{in}} - \sum \dot{E}_{\text{out}} = \dot{W}_P + \dot{E}_D$	(8)
Exergy efficiency	$\varepsilon_p = \frac{\sum_i \dot{E}_i - \sum_e \dot{E}_e}{\dot{W}_p}$	(9)
Heat exchangers		
Energy balance	$\dot{m}_i h_i - \dot{m}_e h_e = 0$	(10)
Exergy destruction	$\sum \dot{E}_{\text{in}} - \sum \dot{E}_{\text{out}} = \dot{E}_D$	(11)
Exergy efficiency	$\mu = \frac{\Delta \dot{E}_{\text{Stream to be heated}}}{\Delta \dot{E}_{\text{Stream used for heating}}}$	(12)
Reactor		
Energy balance	$w_{u\,\max} \cong c_v T_{\text{fiss}} \cong u_{\text{fiss}} = q_{\text{fiss}}$	(13)
Exergy destruction	$\dot{Q}_{\text{fiss}} + \sum_{\text{in}} \dot{E} - \sum_{\text{out}} \dot{E} = \dot{E}_D$	(14)
Exergy efficiency	$\varepsilon_R = \frac{\sum_{\text{out}} E - \sum_{\text{in}} \dot{E}}{\dot{Q}_{\text{fiss}}}$	(15)

Once the power plant and desalination system have all the required parameters, the heat source has to be defined to start the simulation. In this step, DE-TOP allows the user to select the steam extraction points to the desalination plant and the condensate return point from the desalination plant to the power plant. Then, a cogeneration plant is simulated. The two main constraints that limit the possible steam extraction points are (1) the required energy for the desalination plant, which defines the amount of extracted steam, and (2) the desalination technology, which defines the quality of the required heat. Different desalination technologies, such as MED, MSF, and LT-MED, operate at different temperature ranges. Therefore, the temperature of the steam extraction point must be higher than the desalination plant requirements. In this regard, the maximum brine temperature defines the lowest temperature of the steam extraction point. Minimizing the power loss ratio of the power plant can encourage the use of multiple steam extraction points, which allow the system to operate flexibly. All possible steam extraction (red points; A–I) and condensate return (blue points: K–P) points are shown in Fig. 3. The dashboard under the power plant diagram entitled "Select steam extraction parameters" shows the minimum required temperature and target power (written in red). In this case, the required steam flow rate (kg/s) is defined by the user. The selected extraction and condensate return points are shown by a red arrow and a blue arrow, respectively.

Table 2
Main parameters for the power plant predefined cases in DE-TOP V2 [26]

Parameters	PWR (1000)
Steam generator	
Thermal input, Mw(th)	3,002
Live steam pressure, bar	62
Live steam temperature, °C	278
Reheat	
Pressure (HP turbine exhaust), bar	9.9
Temperature, °C	270
Feed water line	
Final feed water temperature, °C	218
Number feed water preheaters	5
Deaerator position in the feed water line	4
Cooling system	
Condensing steam pressure, bar	0.085
Component efficiencies (%)	
Steam generator efficiency	1
Hp turbine efficiency	0.85
Lp/Ip turbine efficiency	0.83
Generator efficiency	0.98
Pump efficiency	0.85
Power plant auxiliary load	0.05
Feed water preheating line (pressure of steam extraction to preheaters) (bar)	
Preheater 1	0.4
Preheater 2	1.5
Preheater 3	4.2
Preheater 4	9.9
Preheater 5	22.3

Table 3
Desalination plant parameters [9]

Parameters	Value
Desalination technology	Multi effect distillation
Desalination plant capacity, m^3/d	50,000
Number of effects	16
Gain output ratio	12.8
Heat needed, Mw(th)	105
Max brine temperature, °C	75
Min required temperature, °C	85.5
Sea water TDS, ppm	35,000

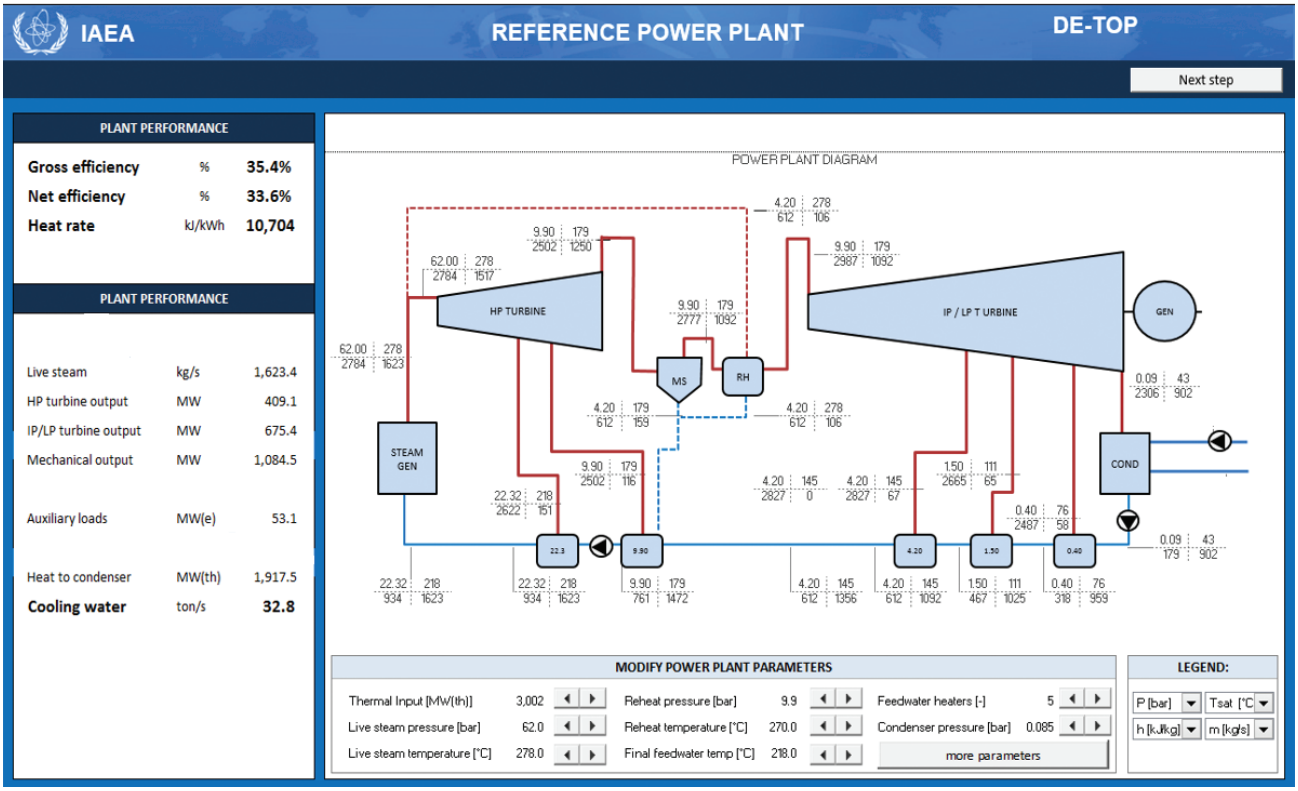

Fig. 2. GUI for the power plant model definition with DE-TOP V2.

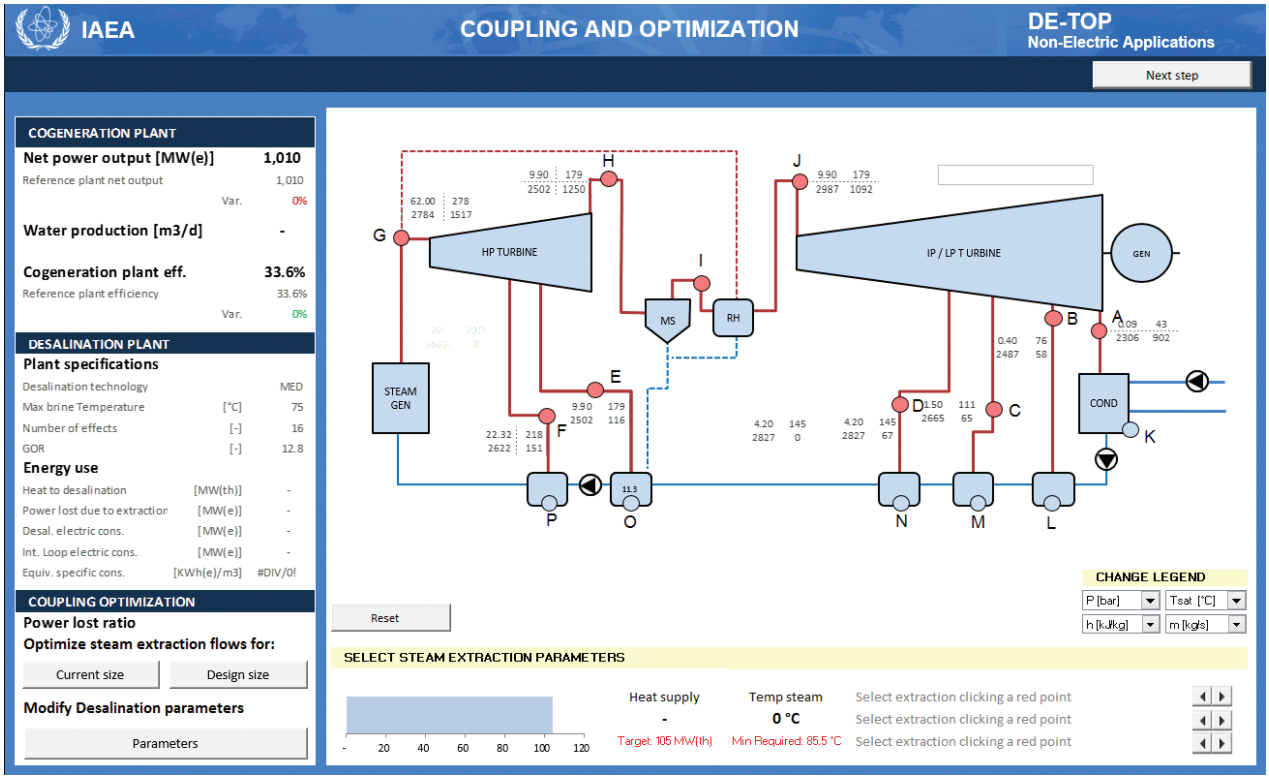

Fig. 3. All possible steam extraction (red points: A–I) and condensate return (blue points: K–P) points. Selected extraction point (red arrow) and return point (blue arrow).

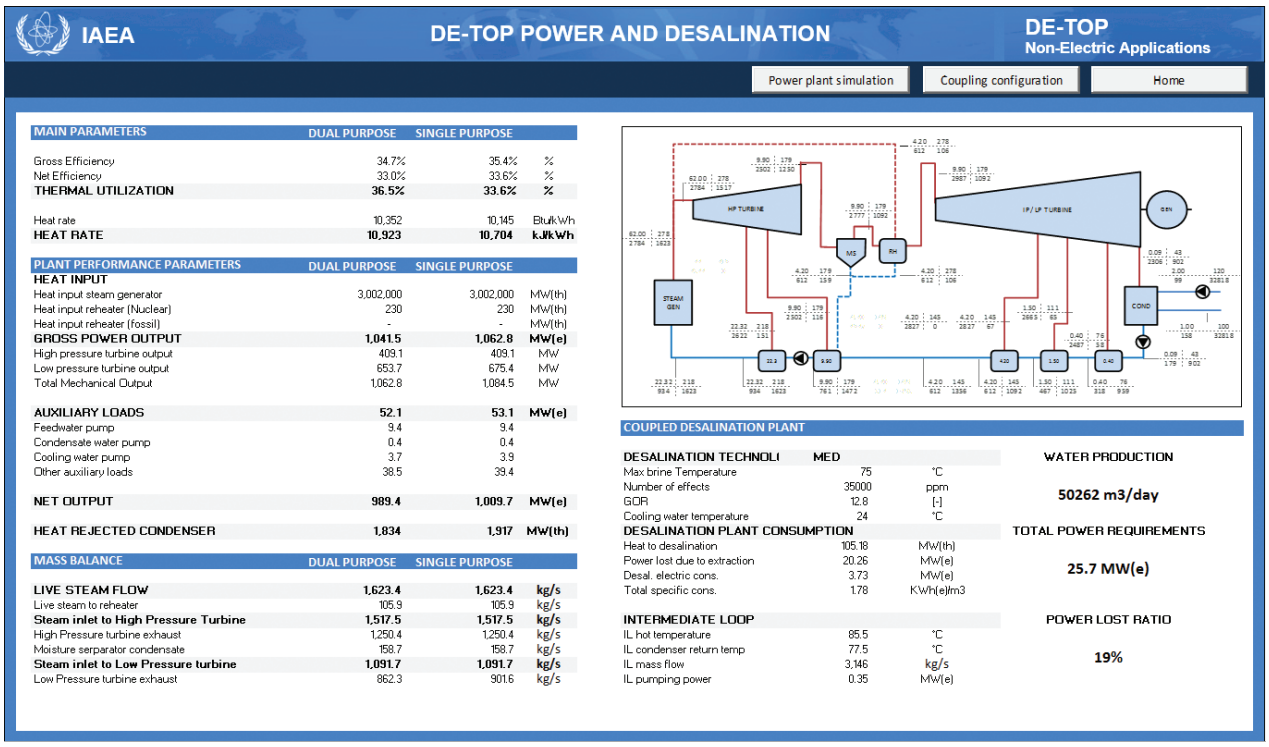

Fig. 4. DE-TOP's final report for the coupled NPP and seawater desalination plant.

Table 4
Benchmarking results for the DE-TOP V2 power plant calculation model

Parameters	REF	DE-TOP V1.0	DE-TOPV 2.0	Error
Gross power output, MW(e)	1,020	1,019	1,062.8	4.2%
Secondary cycle auxiliary loads, MW(e)	N/A	18.8	N/A	[–]
Heat rejected through, MW(th)	N/A	1,954	1,917	[–]
Gross efficiency, %	34.0	33.9	35.4	3.9 %
Feedwater to steam generator, kg/s	1,636.1	1,624	1,623.5	0.8 %
Steam to condenser, kg/s	N/A	911	902	[–]
LP turbine exhaust quality, %	90	89	89	1.1%
Cooling water circulation flow, tn/s	33.4	33.5	32.8	1.8 %

Fig. 4 illustrates a final report sample that shows a list of output parameters, including all performance parameters for single (electricity production) and dual (electrical and thermal production) purposes. Performance parameters include detailed data on the power plant and desalination plant, such as the main parameters of the power plant, plant performance parameters before and after cogeneration, mass balance, and coupled desalination plant [34].

Several parameters are used to compare the performance of different desalination plants. The two most important parameters are the power loss ratio and thermal utilization (TU) factor. The power loss is the difference between the power output of the single electricity production (reference) plant (W_t^{ref}) and the power output of the cogeneration plant (W_t^{cogen}) as shown follows:

$$\Delta w = (W_t^{\text{ref}} - W_t^{\text{cogen}}) \quad (16)$$

The power loss is the amount of heat delivered to the desalination plant. The power loss ratio is further defined as the ratio of power lost to useful heat as follows:

$$\text{Power loss ratio} = (\text{power lost/useful heat}) \quad (17)$$

The TU factor is an important parameter that is generally used to characterize the performance characteristics of a cogeneration plant and shows the enhancement of the overall efficiency of a cogeneration system. The TU factor is the percentage of primary energy utilized by the end user and is described and computed by using DE-TOP as follows:

$$\text{TU} = (W + Q_u)/F \quad (18)$$

where W, Q_u, and F are the work produced by the power plant, the useful heat delivered to the desalination plant, and the energy in the fuel supplied to the dual-purpose plant, respectively [34].

2. Benchmarking

To validate the DE-TOP V2 model, a PWR power plant used in the coupled nuclear desalination plant was simulated for a single purpose on the basis of the parameters listed in Table 1. Results were compared with the experimental and theoretical results (based on the old version DE-TOP V1) in reference 26. Table 4 summarizes the benchmarking results and shows the excellent agreement between the results of the new and old versions of DE-TOP and the experimental results.

3. Results and discussion

All possible coupling configurations between a PWR NPP and MED (with their parameters listed in Tables 2 and 3) were investigated by using DE-TOP V2. The possible configurations are linked points, namely, C–K, C–L, C–M, C–O, D–N, H–O, J–O, J–K, and multi-extraction points of C–M and A–K, and C–M and B–L, where A, B, C, D, H, and J are the steam extraction points and K, L, M, N, and O are the return points. These points were chosen based on the minimum required temperature, target power, and required steam flow rate. The simulation results are shown in Table 5. The important comparative parameters, such as power loss ratio, net efficiency, TU, and total power requirement, noticeably varied from 8.7% to 28.5%, 32.6% to 33.3%, 36.1% to 36.9% and 14.7 to 35.3 MWe, respectively. The minimum power loss ratio, total power requirement, maximum net efficiency, and TU were obtained from multi-extraction points C–M and A–K, which included the heat rejected by the condenser (A–K).

Different scenarios based on possible coupling configurations between the nuclear plant and desalination process are studied to determine the optimum extraction and return points. Initially, the effect of different condensate return points on the coupling configuration performance was studied. In this regard, steam extraction point C is considered the start point, and different condensate return points K, L, M, and O are considered the return points from the MED plant. Figs. 5 and 6 show the net efficiency and power loss ratio of

Table 5
Results of the simulation for different extraction options available in DE-TOP V2

Main parameters					
Parameters	Single	C–K	C–L	C–M	C–O
Gross efficiency, %	35.4	34.8	34.9	34.9	34.9
Net efficiency, %	33.6	33.1	33.1	33.2	33.1
Thermal utilization, %	33.6	36.6	36.6	36.6	36.6
Heat rate, Btu/kWh	10,145	10,307	10,297	10,292	10,295
Heat rate, Kj/kWh	10,704	10,875	10,864	10,859	10,862
Plant performance					
Heat input steam generator, Mw(th)	3,002	3,002	3,002	3,002	3,002
Heat input reheater (nuclear), Mw(th)	230	230	230	230	229
Gross power output, Mw(e)	1,062.8	1,046	1,047.1	1,047.6	1,047.3
Hight pressure turbine output, Mw(e)	409.1	409.1	409.1	409.1	409.2
Low pressure turbine output, Mw(e)	675.4	658.3	659.4	659.9	659.5
Total mechanical output, Mw(e)	1,084.5	1,067.4	1,068.5	1,069	1,068.7
Auxiliary loads, Mw(e)	53.1	52.3	52.4	52.4	52.4
Feed water pump, Mw(e)	9.4	9.4	9.4	9.4	9.1
Condensate water pump, Mw(e)	0.4	0.4	0.4	0.4	0.4
Cooling water pump, Mw(e)	3.9	3.7	3.7	3.7	3.7
Other auxiliary loads, Mw(e)	39.4	38.7	38.8	38.8	39.2
Net output, Mw(e)	1,009.7	993.7	994.7	995.2	994.9
Heat rejected condensate, Mw(th)	1,917	1,816	1,829	1,828	1,829
Desalination plant consumption					
Heat to desalination, Mw(th)	[–]	104.64	104.64	104.64	104.64
Power loss due to extraction, Mw(e)	[–]	15.95	14.94	14.48	14.77
Desal.electric cons, Mw(e)	[–]	3.71	3.71	3.71	3.71
Total specific cons, kWh(e)/ m^3	[–]	1.78	1.78	1.78	1.78
Total power requirements, Mw(e)	[–]	21.4	20.4	19.9	20.2
Power loss ratio, %	[–]	15.2	14.3	13.8	14.1

(*Continued*)

Table 5 (*Continued*)

Main parameters						
Parameters	D–N	H–O	J–O	J–K	C–M,A–k	C–M,B–L
Gross efficiency, %	34.7	34.5	34.5	34.4	35.1	35.1
Net efficiency, %	33.0	32.8	32.8	32.6	33.3	33.3
Thermal utilization, %	36.5	36.3	36.3	36.1	36.9	36.8
Heat rate, Btu/kWh	10,352	10,399	10,408	10,453	10,239	10,242
Heat rate, kj/kWh	10,923	10,972	10,982	11,029	10,803	10,807
Plant performance parameters						
Heat input steam generator, Mw(th)	3,002	3,002	3,002	3,002	3,002	3,002
Heat input reheater (nuclear), Mw(th)	230	220	231	230	230	230
Gross power output, Mw(e)	1,041.5	1,036.8	1,035.9	1,031.4	1,053.1	1,052.7
Hight pressure turbine output, Mw(e)	409.1	410.3	409	409.1	409.1	409.1
Low pressure turbine output, Mw(e)	653.7	647.7	648	643.4	665.6	665.1
Total mechanical output, Mw(e)	1,062.8	1,058.0	1,057	1,052.5	1,074.6	1,074.2
Auxiliary loads, Mw(e)	52.1	51.8	51.8	51.6	52.7	52.6
Feed water pump, Mw(e)	9.4	9.1	9.1	9.4	9.4	9.4
Condensate water pump, Mw(e)	0.4	0.4	0.4	0.4	0.4	0.4
Cooling water pump, Mw(e)	3.7	3.7	3.7	3.7	3.7	3.7
Other auxiliary loads, Mw(e)	38.5	38.7	38.5	38.0	39.1	39.1
Net output, Mw(e)	989.4	985.0	984.1	979.9	1,000.4	1,000.0
Heat rejected condensate, Mw(th)	1,834	1,839	1,840	1,818	1,822	1,823
Desalination plant consumption						
Heat to desalination, Mw(th)	105.18	105.35	105.32	104.65	105.33	105.17
Power loss due to extraction, Mw(e)	20.26	24.71	25.6	29.84	9.28	10.36
Desal.electric cons, Mw(e)	3.73	3.73	3.73	3.71	3.73	3.73
Total specific cons, kWh(e)/ m^3	1.78	1.78	1.78	1.78	1.78	1.78
Total power requirements, Mw(e)	25.7	30.2	31.1	35.3	14.7	15.1
Power loss ratio, %	19.3	23.5	24.3	28.5	8.7	9.2

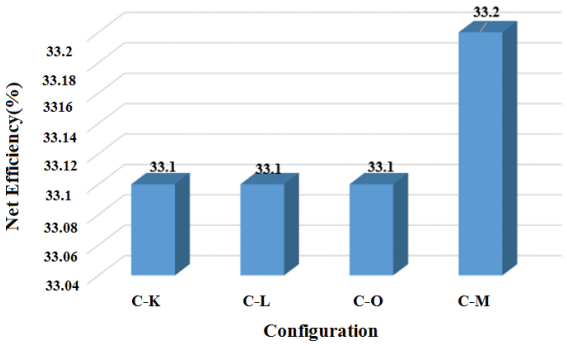

Fig. 5. Net efficiency for four return points (K, L, M, and O) with the same extraction point (C).

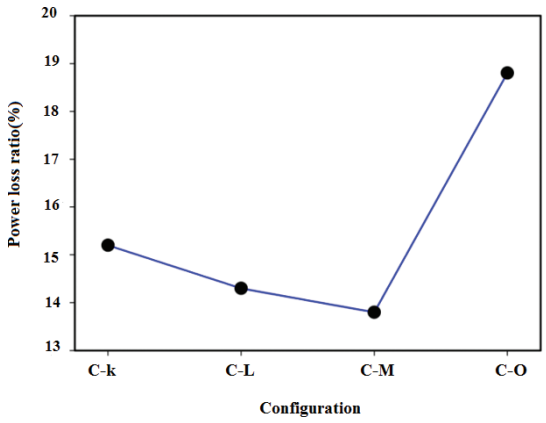

Fig. 6. Power loss ratio for four return points (K, L, M, and O) with the same extraction point (C).

the coupling configuration with an extraction point (C) and different condensate return points (K, L, M, and O), thereby indicating that the maximum net efficiency and the minimum power loss ratio are obtained, where the return point is linked with the pre-heater connected to the extraction point (C), that is, a C–M coupling configuration. Considering that the points after the deaerator are unsuitable for return to the plant, point P is not considered in the simulation.

Second, three steam extraction points (C, D, and J) with different temperatures were considered to study the effect of temperature extraction on the power loss ratio. As shown in Fig. 7, the increased extraction point temperature causes the increase in power loss ratio; this finding agrees with the results of the old version of DE-TOP in [26]. Thus, the second

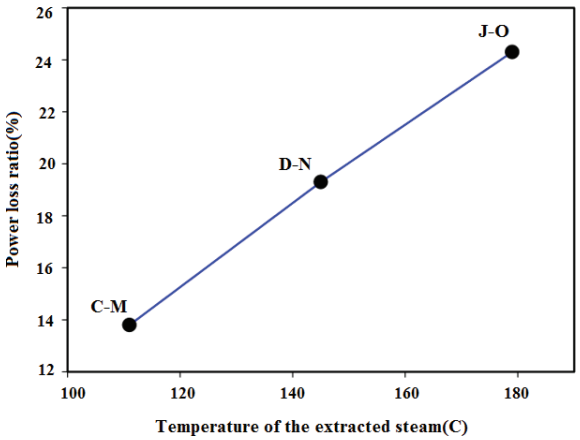

Fig. 7. Effect of extracting temperature on the power loss ratio.

optimization step involves selecting the lowest extraction temperature that is also higher than the minimum required temperature.

One of the steam extraction points that can be used to couple the nuclear plant and the MED processes is the extraction point from the steam flow to the condenser (extraction point: A in Fig. 3). However, its temperature should be higher than the minimum required temperature, that is, the maximum brine temperature of the MED plant. Given that the temperature of point A is lower than the minimum required temperature, it cannot be used solely as an extraction point. Conversely, given the loss in the energy from this point to point K in the condensing process, to prevent energy loss and plant efficiency reduction, it can be used as the multi-extraction point with another extraction point (e.g., A–K and C–M in Table 4). Furthermore, the multi-extraction point is considered to study the effect of using a multi-extraction point on plant efficiency. The temperature and flow rate of each extraction point of the multi-extraction points are listed in Table 6. The final temperature and flow rate of the multi-extraction points are calculated.

Figs. 8–11 show the TU of the dual power plant, the total power requirements, the net efficiency, and the power loss ratio of all possible coupling configurations. As shown in these figures, the parameters have the optimum values for the multi-extraction points. In this regard, the multi-extraction point (C–M and A–K) that uses the condenser stream is the best coupling configuration point and can be suggested to couple the NPP and the MED process. Fig. 12 shows the optimum configuration, which includes the multi-extraction point (C–M and A–K).

In some cases, other desalinization processes, such as MSF and MED-TVC, require higher temperatures. The extraction point temperature of the streams that flow between high-pressure and low-pressure turbines can be appropriate for extraction, such as points H and J in Fig. 3. Different condensate return points, including K, L, M, N, and O, were considered to study the effect of the return point on the power loss ratio. Fig. 13 shows the power loss ratio of the coupling configurations with different condensate return points, thereby indicating that the deaerator return point has the lowest power loss ratio and therefore a higher net efficiency.

Table 6
Temperature, pressure, and flow rate of each extraction points of the multi-extraction points

Configuration C–M, B–L			
Parameters	Flow 1 (C–M)	Flow2 (B–L)	Final Flow
Temperature, °C	111	76	85.9
Flow rate, kg/s	34.7	13.6	48.3
Configuration C–M, A–K			
Parameters	Flow 1 (C–M)	Flow 2 (A–K)	Total Flow
Temperature, °C	111	43	85.9
Flow rate, kg/s	34.7	18	38.5

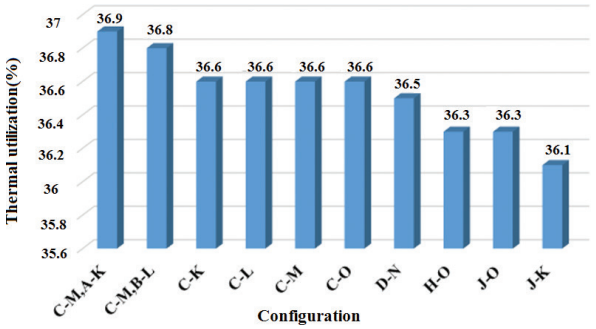

Fig. 8. TU of the dual power plant of all possible coupling configurations.

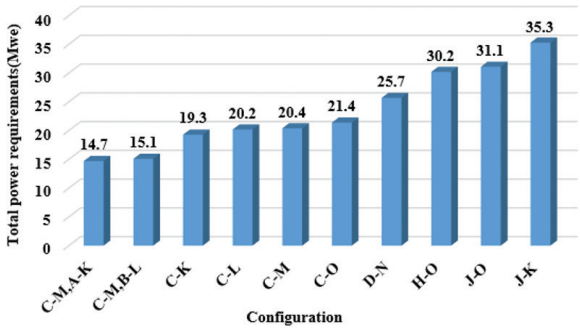

Fig. 9. Total power requirements of all possible coupling configurations.

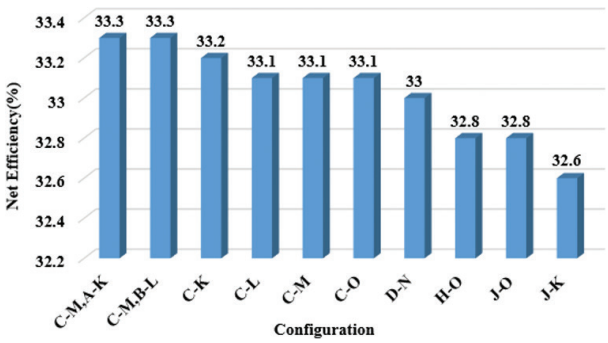

Fig. 10. Net efficiency of all possible coupling configurations.

The steam extraction points H and J located before and after the separator and the re-heater are selected as the extraction point with the same temperature to study the effect of extraction point location on the net output of the power plant. Fig. 14 shows the net output of the power plant for different extraction point positions, thereby indicating that the extraction point H located before the separator and re-heater has a higher net output. This finding can be caused by a reduced thermal load of separator and re-heater.

Fig. 15 shows a diagram of the energy balance of all selected coupling configurations, including gross electrical output, heat to desalination plant, and heat-rejected condensate. Results indicate that the optimum coupling configuration (C–M and A–K) provides the highest gross electrical output.

Table 7 summarizes the values of exergy efficiency and exergy destruction for each component of the power plant.

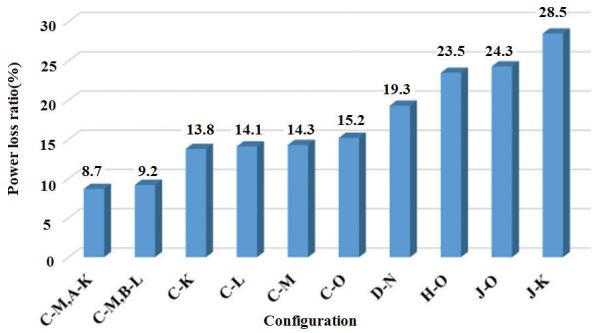

Fig. 11. Power loss ratio of all possible coupling configurations.

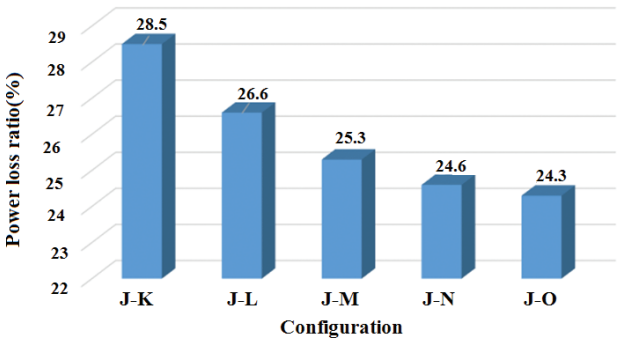

Fig. 13. Power loss ratio of the coupling configurations with different condensate return points.

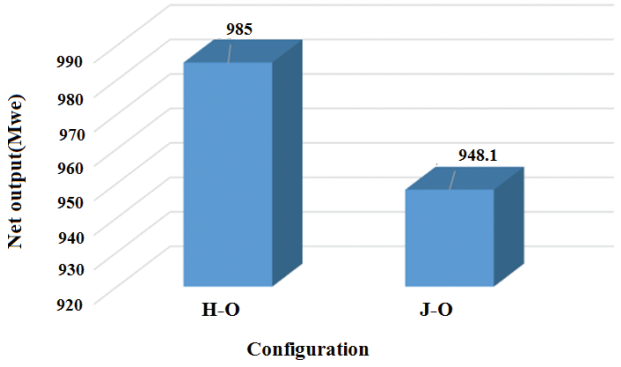

Fig. 14. Net output of the power plant for different extraction point positions.

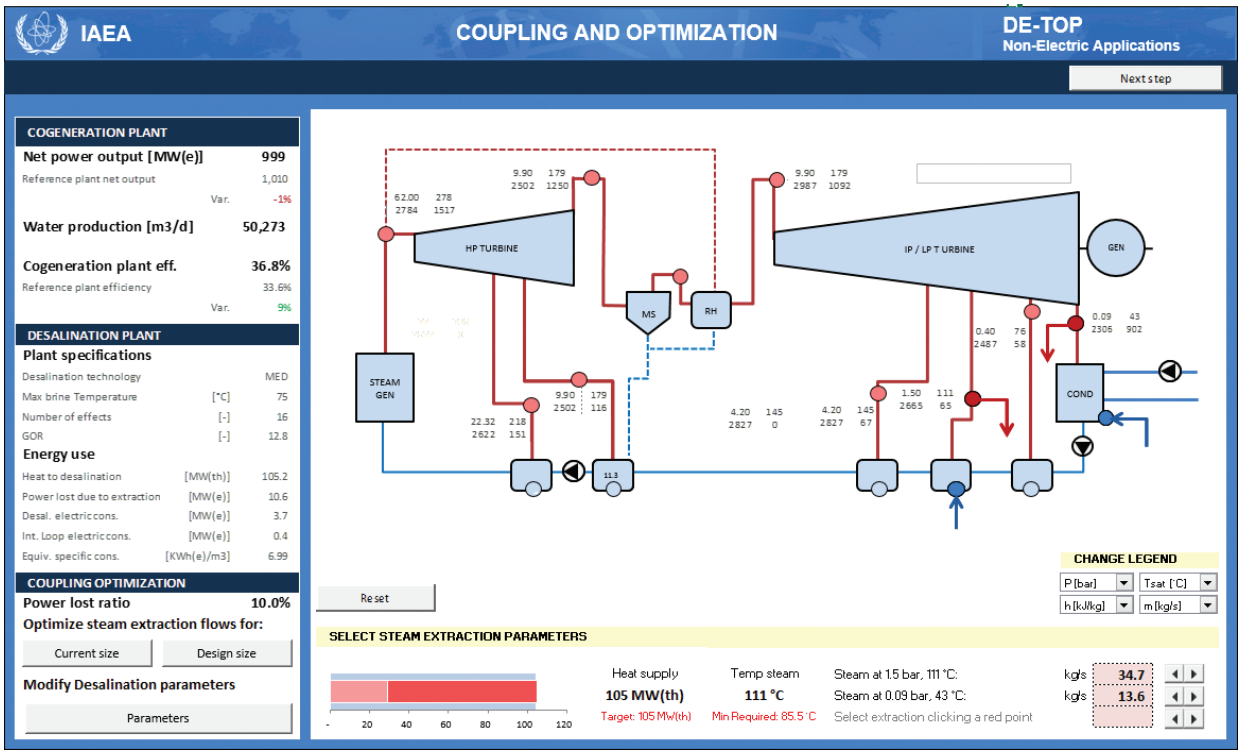

Fig. 12. Optimum configuration that includes the multi-extraction point (C–M and A–K).

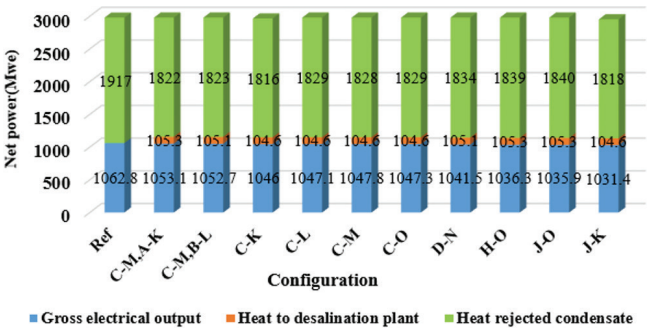

Fig. 15. Energy balance diagram of all selected coupling configurations.

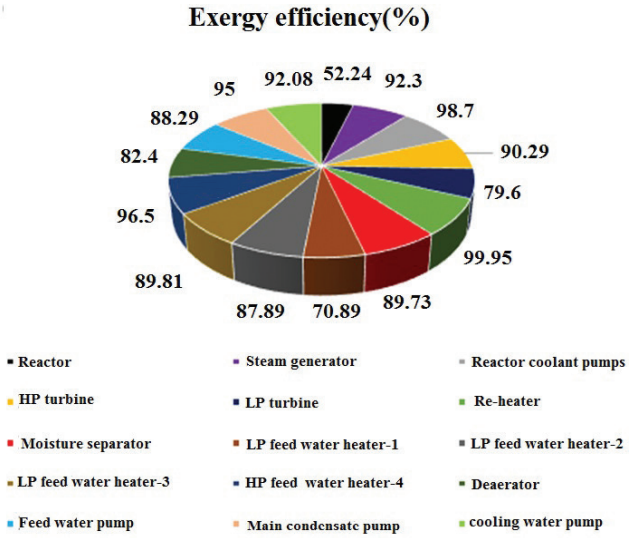

Fig. 16. Exergy efficiency for the power plant components.

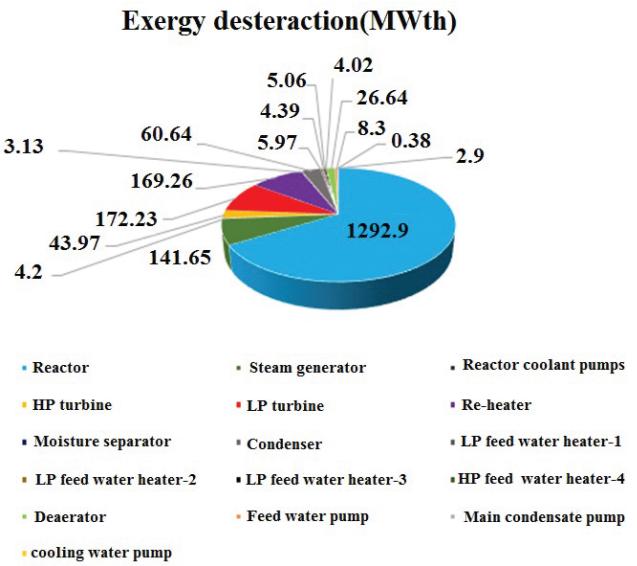

Fig. 17. Exergy destruction for the power plant components.

Table 7
Important parameters of the result from the exergy analysis

Component	Actual work (MWth)	Reversible work (MWth)	Exergy destruction (MWth)	Exergy efficiency (%)
Primary section				
Reactor	1,709.1	3,002	1,292.9	52.24
Steam generators	0	14.86	141.65	92.3
Reactor coolant pumps	–8.32	–4.12	4.2	98.7
			1,437.75	
Power production section				
HP turbine	409.1	453.076	43.976	90.29
LP turbine	675.4	847.630	172.23	79.6
Re-heater	0	169.26	169.26	99.95
Moisture separator	0	3.13	3.13	89.73
			388.59	
Condensation section				
Condenser	0	60.64	60.64	–
			60.64	
Preheating section				
LP feed water heater-1	0	5.97	5.97	70.89
LP feed water heater-2	0	4.39	4.39	87.89
LP feed water heater-3	0	5.06	5.06	89.81
HP feed water heater-4	0	4.62	4.62	96.5
Deaerator	0	2.64	26.64	82.4
Feed water pump	–9.4	–1.1	8.3	88.29
Main condensate pump	–0.4	–0.02	0.38	95.0
Cooling water pump	–3.7	–0.8	2.9	92.08
			58.26	
Network output			1,051.7	
Imbalance			5.06	
TOTAL			3,002	

The highest irreversibility (exergy destruction) evidently belongs first to the reactor and next to the low-pressure turbine. The lowest exergy destruction occurs in the cooling water pump. The exergy efficiency and exergy destruction of components are compared in Figs. 16 and 17, respectively. These figures clearly show that the reactor is responsible for the highest exergy destruction ratio in the power plant. The figures indicate that almost half of the fuel exergy is destroyed in the reactor because of the high irreversibility of the fission process. Figs 18 and 19 show the simplified energy and exergy flows of the power plant. In these figures, the losses due to the heat transfer processes are specified.

4. Conclusion

This study presented a thermodynamic evaluation of a nuclear desalination plant, including the coupling of a pressurized water reactor and a multi-effect distillation system. A simulation study was performed by using a new version of DE-TOP. For exergy analysis, exergy equations were added to the simulator. According to the analysis, the main exergy destructions occur in the reactor core (1,292.9 MWth) and the low-pressure turbine (172.23 MWth). Therefore, they have the lowest exergy efficiency of 52.24% and 79.6%, respectively. Although, other components contribute to the irreversibility of the energy transformation, the reactor is the main source of entropy generation. This condition means that upgrading the core technology could improve the exergy efficiency of the power plant. Coupling configurations between the NPP and the desalination process were developed based on the minimum required temperature, target power, and required steam flow rate. All possible coupling configurations between the steam extraction and the condensate return points were studied. Several important output parameters, including power loss ratio, net efficiency, TU, and total power requirement, that were used to compare the efficiency of the power plant were studied. Results showed that these parameters varied from 8.7% to 28.5%, 32.6% to 33.3%, 36.1% to 36.9% and 14.7 to 35.3 MWe, respectively. The results further indicated that the minimum power loss ratio, total power requirement, maximum net efficiency, and maximum TU were obtained from multi-extraction points, which included the heat rejected by the condenser. Results also indicated that these parameters are strongly dependent on the temperature and position of steam extraction and condensate return points and their coupling type.

Acknowledgment

The support from Shahid Beheshti University is gratefully acknowledged.

Symbols

DEEP	–	Desalination Economic Evaluation Program
DE-TOP	–	Desalination thermodynamic optimization program
e	–	Exit, outflow
$\dot{E}$	–	Total energy flow rate, kW
$\dot{E}_D$	–	Rate of irreversibility, kW
$\dot{E}_X$	–	Total exergy flow rate, kW
$\dot{E}_F$	–	Exergy flow rate of fuel, kW
Ex	–	Exergy, kJ/kg
fis	–	Fission
GUI	–	Graphical user interface
g	–	Gravitational acceleration, 9.8, m/s^2
H	–	Enthalpy, kJ/kg
HPH	–	High pressure feed water heater
HPT	–	High pressure turbine
i	–	Inlet, inflow
IAEA	–	International Atomic Energy Agency
LP	–	Low pressure feed water heater
LPT	–	Low pressure turbine
$\dot{m}$	–	Mass flow rate, kg/s
MED	–	Multi effect distillation
MSF	–	Multi-stage flash
p	–	Pressure, Pa, bar
PWR	–	Pressurized water reactor
RO	–	Reverse osmosis
S	–	Entropy, kJ/kg K
SG	–	Steam generator
T	–	Temperature K, °C
TDS	–	Total dissolved solids
TVC	–	Thermo vapor compressore
TU	–	Thermal utilization
th	–	Thermal
u	–	Specific internal energy, kJ/kg
V	–	Velocity, m/s

References

[1] D. Brogioli, F. La Manti, N.Y. Yip, Thermodynamic analysis and energy efficiency of thermal desalination processes, Desalination, 428 (2018) 29–39.
[2] C.H. Woo, Research trend of membranes for water treatment by analysis of patents and papers' publications, Desal. Water. Treat., 10 (2018) 201–220.
[3] H.S. Kim, H.C. No, Thermal coupling of HTGRs and MED desalination plants, and its performance and cost analysis for nuclear desalination, Desalination, 303 (2012) 17–22.
[4] Y.H. Jung, Y.H. Jeong, J. Choi, A.F.Wibisono, J.I. Lee, H.C. No, Feasibility study of a small-sized nuclear heat-only plant dedicated to desalination in the UAE, Desalination, 336 (2014) 83–97.
[5] M.Y. Park, E.S. Kim, Thermodynamic evaluation on the integrated system of VHTR and forward osmosis desalination process, Desalination, 337 (2014) 117–126.
[6] International Atomic Energy Agency, TECDOC-1561-Economics of Nuclear Desalination: New Developments and Site Specific Studies, Printed by the IAEA, Austria, 2007.
[7] S. Zhou, Y. Guo, X. Mu, S. Shen, Effect of design parameters on thermodynamic losses of the heat transfer process in LT-MEE desalination plant, Desalination, 375 (2015) 40–47.
[8] Y. Bouaichaoui, A. Belkaid, S.A. Amzert, Economic and safety aspects in nuclear seawater desalination, Procedia. Eng., 33 (2012) 146–154.
[9] M.G. Abdoelatef, R.M. Field, Y.-K. Lee, Thermodynamic evaluation of coupling APR1400 with a thermal desalination plant, Int. J. Chem. Molec. Nucl. Mater. Metal. Eng., 9 (2015) 1070–1078.
[10] A.K. Adak, P.K. Tewari, Technical feasibility study for coupling a desalination plant to an advanced heavy water reactor, Desalination, 337 (2014) 76–82.
[11] International Atomic Energy Agency, TECDOC 1524- Status of Nuclear Desalination in IAEA Member States, Printed by the IAEA, Austria, 2007.

[12] G. Amy, N. Ghaffour, Z. Li, L. Francis, R.V. Linares, T. Missimer, S. Lattemann, Membrane-based seawater desalination: present and future prospects, Desalination, 401 (2017) 16–21.
[13] S.U.-D. Khan, S. Haider, A. El-Leathy, U.A. Rana, S.N. Danish, R. Ullah, Development and techno-economic analysis of small modular nuclear reactor and desalination system across Middle East and North Africa region, Desalination, 406 (2017) 51–59.
[14] A. Ahmad, M.V. Ramana, Too costly to matter: economics of nuclear power for Saudi Arabia, Energy, 69 (2014) 682–694.
[15] A Rezaei, A Naserbeagi, G Alahyarizadeh, M Aghaie, Economic evaluation of Qeshm island MED-desalination plant coupling with different energy sources including fossils and nuclear power plants, Desalination, 422 (2017) 101–112.
[16] International Atomic Energy Agency, TECDOC-1056- Nuclear heat applications: design aspects and operating experience, Printed by the IAEA, Austria, 1998.
[17] International Atomic Energy Agency, Hydrogen as an energy carrier and its production by nuclear power, Printed by the IAEA, Austria, 1999.
[18] K. Ansari, H. Sayyaadi, M. Amidpour, Thermoeconomic optimization of a hybrid pressurized water reactor (PWR) power plant coupled to a multi effect distillation desalination system with thermo-vapor compressor (MED-TVC), Energy, 35 (2010) 1981–1996.
[19] International Atomic Energy Agency (IAEA), TECDOC-666- Technical and economic evaluation of potable water production through desalination of seawater by using nuclear energy and other means, Printed by the IAEA, Austria, 1992.
[20] International Atomic Energy Agency (IAEA), TECDOC-1186- Examining the economics of seawater desalination using the DEEP code, Printed by the IAEA, Austria, 2000.
[21] International Atomic Energy Agency (IAEA), TECDOC-1235- Safety aspects of nuclear plants coupled with seawater desalination units, Printed by the IAEA, Austria, 2001.
[22] International Atomic Energy Agency (IAEA), TECDOC-940- Floating nuclear energy plants for seawater desalination, Printed by the IAEA, Austria, 1997.
[23] International Atomic Energy Agency (IAEA), TECHNICAL REPORTS SERIES No. 400-introduction of nuclear desalination, Printed by the IAEA, Austria, 2000.
[24] International Atomic Energy Agency (IAEA), TECDOC-1444- Optimization of the coupling of nuclear reactors and desalination systems, Printed by the IAEA, Austria, 2005.
[25] International Atomic Energy Agency (IAEA), TECDOC-1584- Advanced Applications of Water Cooled Nuclear Power Plants, Printed by the IAEA, Austria, 2008.
[26] I.G. Sánchez-Cervera, K.C. Kavvadias, I. Khamis, DE-TOP: a new IAEA tool for the thermodynamic evaluation of nuclear desalination, Desalination, 321 (2013) 103–109.
[27] F. Hafdhi, T. Khir, A. Ben Yahia, A. Ben Brahim, Exergoeconomic optimization of a double effect desalination unit used in an industrial steam power plant, Desalination, 438 (2018) 63–82.
[28] A. Hosseini, A. Banakar, S. Gorjian, Development and performance evaluation of an active solar distillation system integrated with a vacuum-type heat exchanger, Desalination, 435 (2018) 45–59.
[29] T. Ming, T. Gong, R.K. de Richter, C. Cai, S.A. Sherif, Numerical analysis of seawater desalination based on a solar chimney power plant, Appl. Energy., 208 (2017) 1258–1273.
[30] G. Alonso, S. Vargas, E. del Valle, R. Ramirez, Alternatives of seawater desalination using nuclear power, Nucl. Eng. Design., 245 (2012) 39–48.
[31] S. Dincer, I. Dincer, Comparative evaluation of possible desalination options with various nuclear power plants, Exerg. Energ. Environ. Dimen., (2018) 569–582.
[32] N.Y. Mansouri, A.F. Ghoniem, Does nuclear desalination make sense for Saudi Arabia, Desalination, 406 (2017) 37–43.
[33] W. Li, Y. Zhang, W. Zheng, Investigation on three seawater desalination processes coupled with NHR-200, Desalination, 298 (2012) 93–98.
[34] International Atomic Energy Agency, DE-TOP User's Manual Version 2.0 Beta, 2014.
[35] A.M. Elaskary, System simulation for coupling nuclear power plants and desalination in different scenarios, Int. J. Scient. Eng. Res., 4 (2013) 1116.
[36] International Atomic Energy Agency (IAEA), TECDOC-942- Thermodynamic and economic evaluation of co-production plants for electricity and potable water, Printed by the IAEA, Austria, 1997.
[37] A Naserbegi, M Aghaie, A Minuchehr, G Alahyarizadeh, A novel exergy optimization of Bushehr nuclear power plant by gravitational search algorithm (GSA), Energy, 148 (2018) 373–385.
[38] R. Terzi, I. Tukenmez, E. Kurt, Energy and exergy analyses of a VVER type nuclear power plant, Int. J. Hydrogen. Energy., 41 (2016) 12465–12476.
[39] H. Sayyaadi, T. Sabzaligol, Exergoeconomic optimization of a 1000 MW light water reactor power generation system, Int. J. Energy. Res., 33 (2009) 378–395.